

Analysis and Simulation of Beam-Beam Effects in a Linac-Ring Collider

R. Li, K. Beard, J. Boyce, G. Krafft, L. Merminga, B. C. Yunn

Jefferson Lab

V. Lebedev

Fermilab

J. J. Bisognano

SRC, Univ. Wisconsin-Madison



- Introduction
- Strong-Strong Beam-Beam Simulation
- Analysis of the Beam-Beam Kink Instability in the Linac-Ring B Factory
- Strong Head-Tail Instability in a Linac-Ring e-p Collider
- Summary

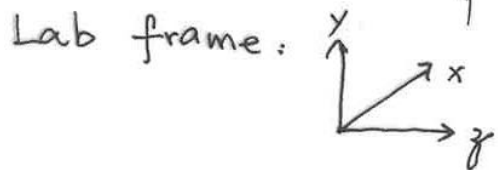
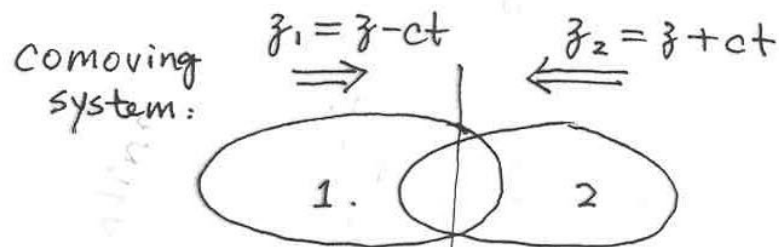


Operated by the Southeastern Universities Research Association for the U.S. Dept. of Energy

1. Introduction

Luminosity : reaction events produced by unit reaction cross section area

$$\mathcal{L} = zc f_c \int n_1(x, y, z - ct) n_2(x, y, z + ct) d^3\vec{r} dt$$



$$\mathcal{L} = \frac{N_+ N_- f_c}{2\pi \sqrt{\sigma_{x+}^2 + \sigma_{x-}^2} \sqrt{\sigma_{y+}^2 + \sigma_{y-}^2}} \quad (\text{Gaussian bunches})$$

Desired Luminosity $> 10^{33} \text{ cm}^{-2} \text{s}^{-1}$

Linear Beam-Beam Tune Shift (ring-ring)

For e^+e^- collider, focusing force on a particle in e^+ beam due to the interaction of opposing e^- beam is:

$$F_{y+} = e(1+\beta^2) \frac{\partial V(x,y)}{\partial y} \approx -\frac{2N_e e^2 y}{\sigma_{y-}(\sigma_{x-} + \sigma_{y-})} \quad (y \ll \sigma_y, \beta \rightarrow 1)$$

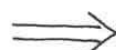
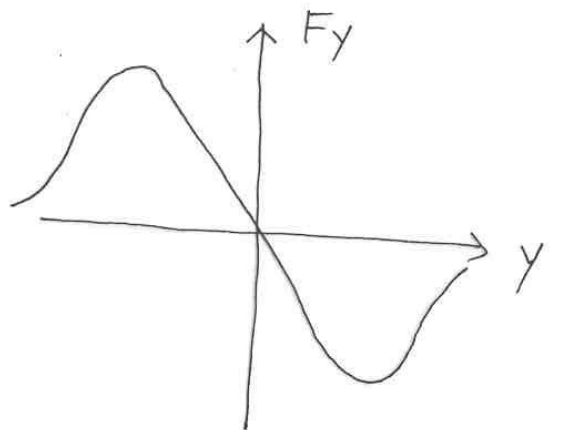
$$\left(\nabla^2 V = 4\pi \rho, \quad \rho(x,y) = \frac{N_e e}{2\pi \sigma_{x-} \sigma_{y-}} e^{-\frac{x^2}{2\sigma_{x-}^2} - \frac{y^2}{2\sigma_{y-}^2}} \right)$$

$$M = \begin{bmatrix} 1 & 0 \\ -\frac{1}{f_{y+}} & 1 \end{bmatrix} \begin{bmatrix} \cos 2\pi \gamma_y & \beta_{y+}^* \sin 2\pi \gamma_y \\ -\frac{1}{\beta_{y+}^*} \sin 2\pi \gamma_y & \cos 2\pi \gamma_y \end{bmatrix}, \quad \frac{1}{f_{y+}} = \frac{2N_e r_0}{\gamma + \sigma_{y-}(\sigma_{x-} + \sigma_{y-})}$$

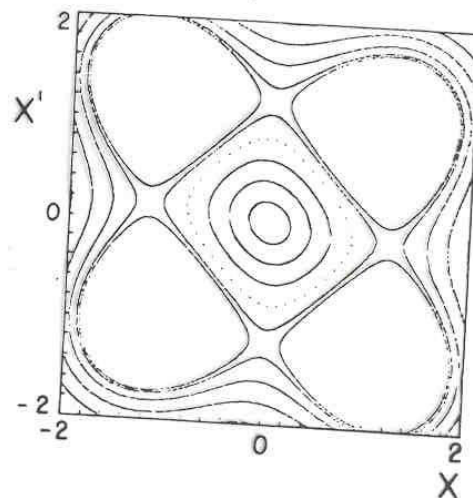
$$\cos 2\pi(\gamma_{y+} + \beta_{y+}) = \frac{1}{2} \text{Tr } M$$

$$\beta_{y+} = \frac{r_0 N_e \beta_{y+}^*}{2\pi \gamma_+ \sigma_{y-} (\sigma_{x-} + \sigma_{y-})} \quad (y \leftrightarrow x, + \leftrightarrow -)$$

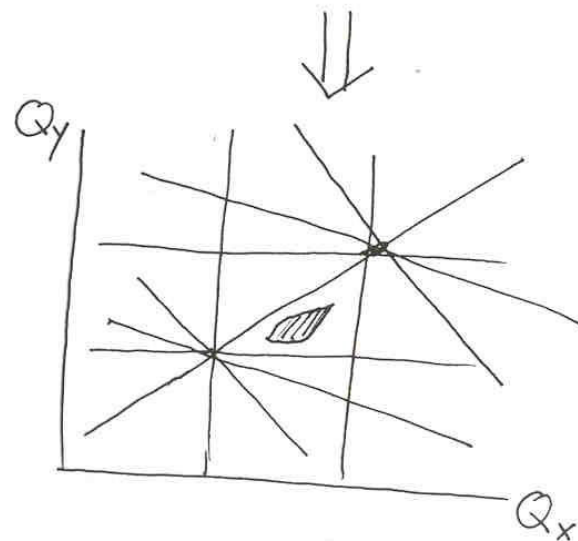
Beam - Beam Tune shift Limit (nonlinear effect)



$$\beta_y \propto \frac{F_y}{y} \text{ amplitude dependent}$$



islands and separatrix



working area

Observed Limit (diffusion)

$$\beta < 0.05$$

(e⁺e⁻ ring)

Motivation for Linac-Ring Colliders

[Grosse-Wiesmann]

e^-e^+ collider

<Advantages>

Ring-Ring

- economic

Linear Collider

- No SR
- No $\beta_{x,y}$ limit

Linac-Ring

- two machines relatively decoupled (?)
- accumulation of e^+

<disadvantages>

- E_{cm} limited by SR
- L limited by $\beta_{x,y}$
- e^+ production and damping
- beamstrahlung

- lower $N_- \Rightarrow$ low $\alpha_{x,y}$
lower γ_-
high $\frac{N_+}{\alpha_{x,y}}$



high disruption of e^-

Disruption

e^- being focused by the e^+ beam

$$D_{y-} = \frac{D_{z+}}{f_{y-}} = \frac{2N_+ r_0 D_{y+}}{\gamma_- D_{y+} (\delta_{x+} + \delta_{y+})}$$

$D_{y-} \gg 1 \Rightarrow$ electrons oscillate through the positron bunch

- Special Feature of Beam-Beam Interaction in a Liniac-ring collider:
 - stored bunch collides with highly disrupted e^- bunch
 - need strong-strong simulation to study the evolution of the strong (e^+) beam in the process of interaction with the highly disrupted weak (e^-) beam.
 - e^- acts as active impedance
 - jitter in linear beam

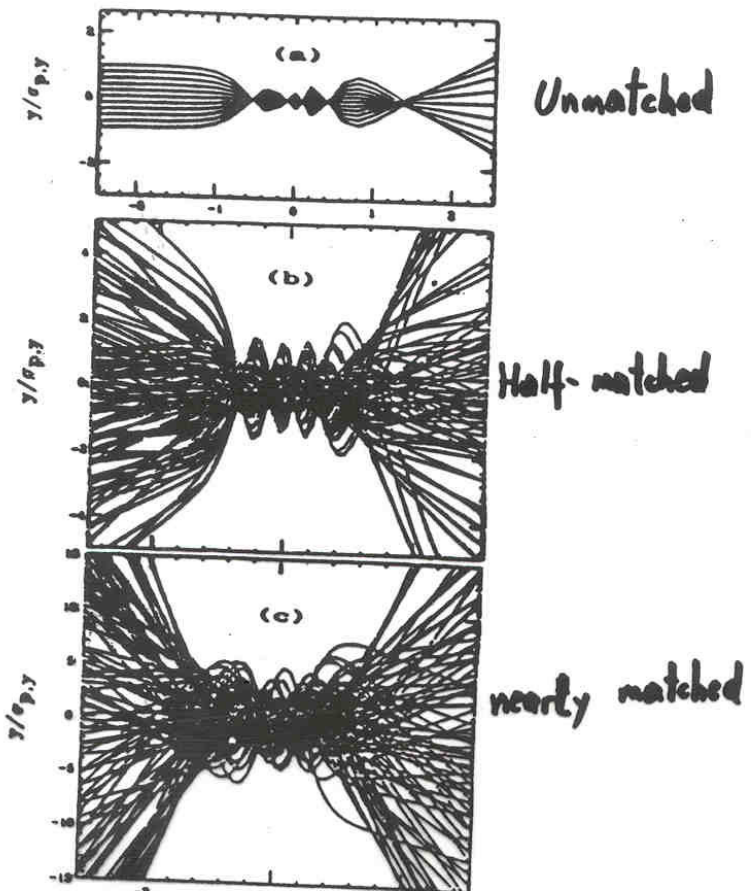


Figure 2. The trajectories of individual electrons traveling from left to right through a positron bunch are plotted with respect to the center of mass of the positron bunch. The positron bunch extends from -1 to +1 along the abscissa. (a) Individual electrons with parallel trajectories colliding with a strong positron bunch exhibit localised pinching or foci. (b) Colliding electrons with more realistic pre-collision trajectories also show the pinching effects, though not as strong. (c) Electron trajectories after bunch optics have been "matched" according to the procedure discussed in Ref. 5. The foci have been reduced significantly.

All offsets were bunched v calculated.

Figure with no π and negative shows the plotted in bunch. Figure each slice, Figure 4b It is clear it tend to dis-

Figure Figure 5a are for x z calculation 6 but match

The a any detect a minimum macroparti these resul further stu before any

Finall is shown in the lumin (For all of $4 \times 10^{34} \text{ cm}^{-2}$

2. Strong-Strong Beam-Beam Simulation

- (1) about the code
- (2) beam-beam in a ring-ring B factory
- (3) beam-beam in a linac-ring B factory

(1) About the code

Beam- Beam Interaction

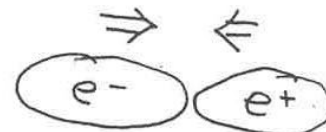
bunch



slice



macroparticles



Interaction Region

- Bunches are modeled by transverse slices populated with finite number of macroparticles with finite size
- Elliptical macroparticles are Gaussian in $x-y$ plane
$$R^{(\text{macro})} = \frac{\sigma_x^{(\text{macro})}}{\sigma_y^{(\text{macro})}} \approx R^{(\text{bunch})}$$
- During collision, only macroparticles in overlapping slices experience mutual forces

Force Calculation

$$\vec{F}(\vec{r}_i^{(+)}) = \sum_m \vec{f}(\vec{r}_i^{(-)} - \vec{r}_m^{(+)})$$

For Gaussian distribution,

$$P_m(x, y) = \frac{n_m e}{2\pi \sigma_{mx} \sigma_{my}} \exp\left(-\frac{x^2}{2\sigma_{mx}^2} - \frac{y^2}{2\sigma_{my}^2}\right) \quad \begin{cases} \nabla^2 \phi = P_m/e \\ \vec{E} = -\vec{\nabla} \phi \end{cases}$$

- Field in terms of Complex error function [Bassetti & Erskine].

$$(E_x, E_y) = \frac{n_m e}{2\epsilon_0 \sqrt{2\pi(\sigma_{mx}^2 - \sigma_{my}^2)}} (I_m \Xi, R_m \Xi)$$

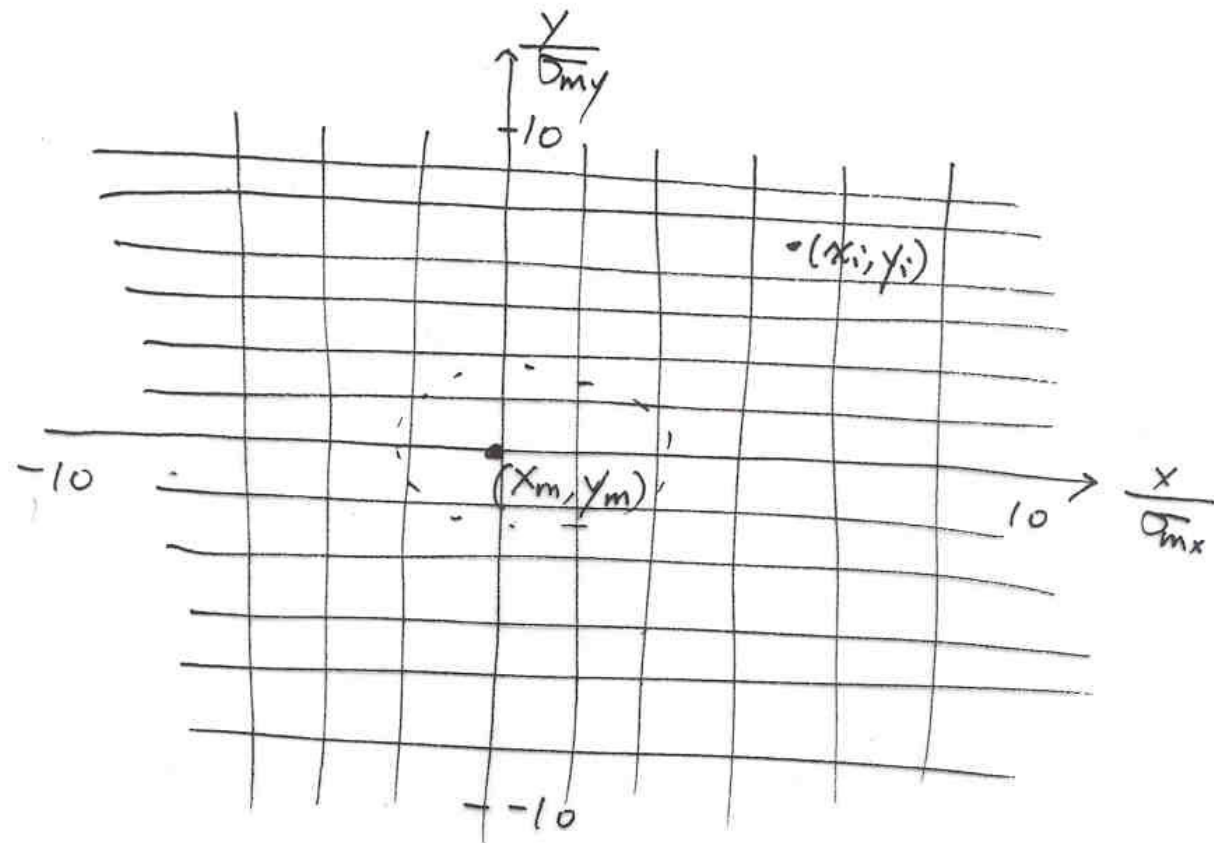
with $\Xi = W\left(\frac{x+iy}{\sqrt{2(\sigma_{mx}^2 - \sigma_{my}^2)}}\right) - e^{-\frac{x^2}{2\sigma_{mx}^2} - \frac{y^2}{2\sigma_{my}^2}} W\left(\frac{x\frac{\sigma_{my}}{\sigma_{mx}} + iy\frac{\sigma_{mx}}{\sigma_{my}}}{\sqrt{2(\sigma_{mx}^2 - \sigma_{my}^2)}}\right)$

$$W(z) = e^{-z^2} \operatorname{erfc}(-iz)$$

- Use lookup table for $f_{x,y}\left(\frac{x_i - x_m}{\sigma_{mx}}, \frac{y_i - y_m}{\sigma_{my}}, R = \frac{\sigma_{mx}}{\sigma_{my}}\right)$

- Luminosity $L_{\text{total}} = \sum_{i,m} L^{(im)}$

- Lookup table for force calculation



given aspect ratio

Noise Consideration

choice of $\sigma_{mx,y}$ and N_m

macroparticle model:

$$\rho(\vec{x}, t) = \int d\vec{x}' S(\vec{x} - \vec{x}') \rho_c(\vec{x}', t)$$

Fourier transform

$$\tilde{\rho}(\vec{k}, t) = \hat{S}(\vec{k}) \tilde{\rho}_c(\vec{k}, t)$$

Gaussian macroparticle

$$q_m e^{-\frac{k_x^2 \sigma_{mx}^2}{2} - \frac{k_y^2 \sigma_{my}^2}{2}}$$

Gaussian centroid distribution

$$N_m e^{-\frac{k_x^2 \sigma_{Bx}^2}{2} - \frac{k_y^2 \sigma_{By}^2}{2}}$$

Effective rms bunch size

$$\sigma_{Bx}^{eff} = \sqrt{\sigma_{Bx}^2 + \sigma_{mx}^2}, \quad \sigma_{By}^{eff} = \sqrt{\sigma_{By}^2 + \sigma_{my}^2}$$

\Rightarrow smooth and realistic representation requires

$$\left(\frac{\sigma_{mx,y}}{\sigma_{Bx,y}} \right)^2 \ll 1 \quad (\text{realistic})$$

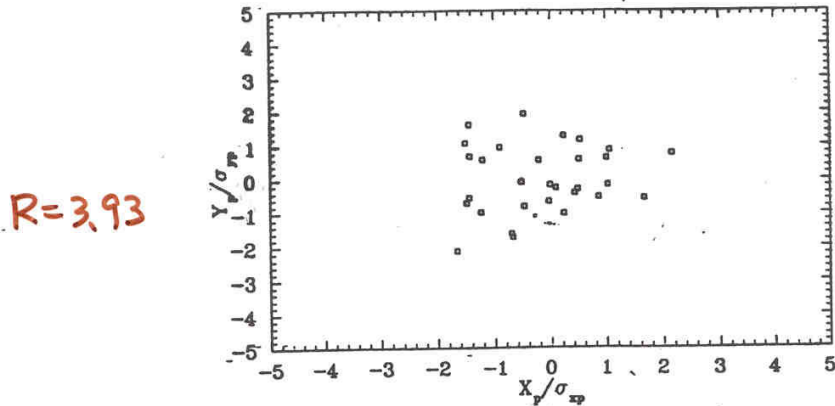
$$N_m \gg N_0 = \frac{\sigma_{Bx} \sigma_{By}}{\sigma_{mx} \sigma_{my}} \quad (\text{overlap})$$

Example:

$$\frac{\sigma_{mx}}{\sigma_{Bx}} = \frac{1}{2},$$

$$\sigma_{Bx}^{eff} \approx 1.12 \sigma_{Bx}$$

Force calculated using macro-particle mode



center of 30 macroparticles simulating a Gaussian slice

Figure 1: Transverse distribution of 30 macro-particle in e+ bunch

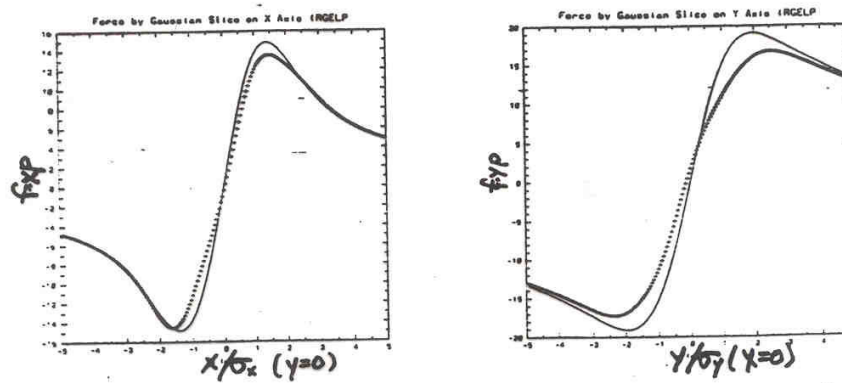
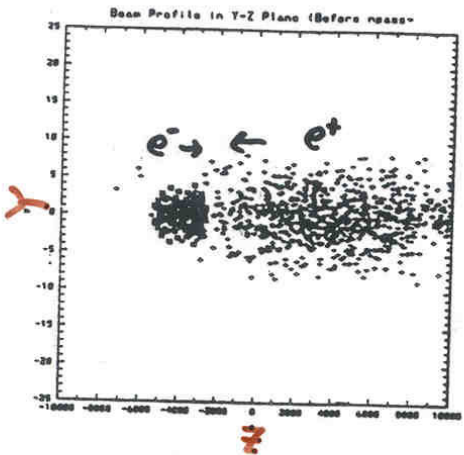


Figure 2: Force calculated by macro-particle model (dotted curves) compared to analytical results (solid curves)

$$\frac{\sigma_{mx,y}}{\sigma_{bx,y}} = \frac{1}{2}.$$

Comparison of Results obtained using different number of macro particles

$$N_m^- = 360, \quad N_m^+ = 1000$$



RHYP vs. NTURN (RGELPS.FI)

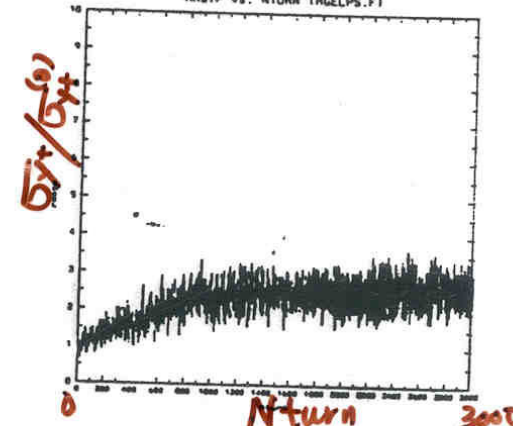
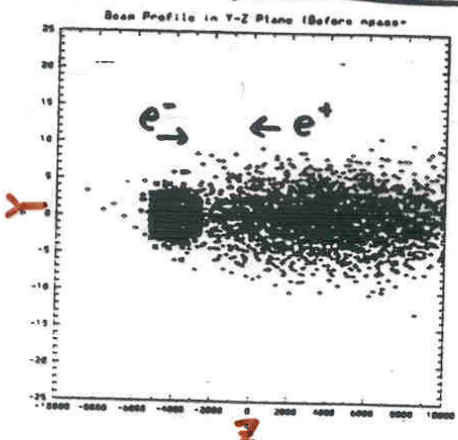


Figure 1: Beam profiles after 3000 collision ($N_e = 360, N_p = 1000$)

Figure 3: Positron beam blowup after 3000 collision ($N_e = 360, N_p = 1000$)

$$N_m^- = 1440, \quad N_m^+ = 4000$$



RHYP vs. NTURN (RGELPS.FI)

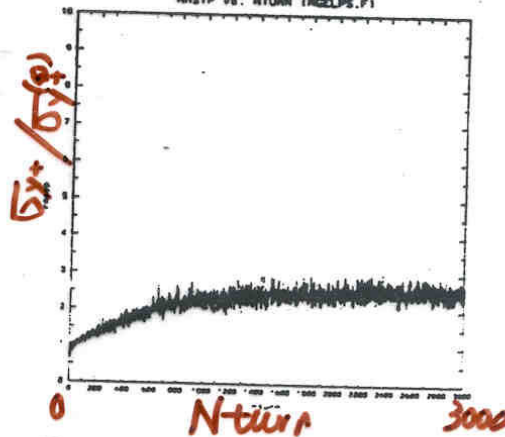
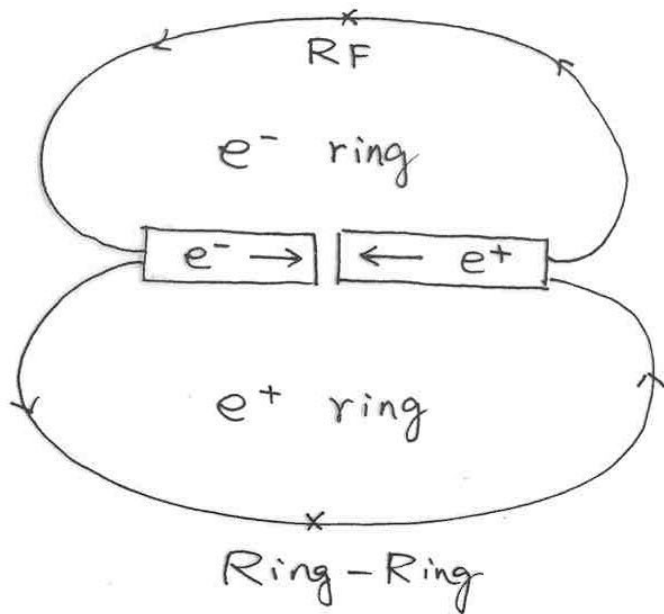


Figure 2: Beam profiles after 3000 collision ($N_e = 1440, N_p = 4000$)

Figure 4: Positron beam blowup after 3000 collision ($N_e = 1440, N_p = 4000$)

Layout of the Program



Linac - Ring

Beam Dynamics Includes:

- Beam - Beam Interaction at IR
- Linear Matrix in the Ring
- Transverse: damping due to RF, and quantum excitation
- Longitudinal: synchrotron oscillation, radiation damping, quantum excitation

(2) Ring-Ring Beam-Beam Effects

Simulation

benchmark with existing beam-beam results in a ring-ring B factory

of macro-particles in each bunch = 300

slices in each bunch = 5

macroparticle size $\frac{\sigma_{mx,y}}{\sigma_{bx,y}} = 0.5$

Aspect ratio $R = \frac{\sigma_{mx}}{\sigma_{my}} = \left(\frac{\sigma_{bx}}{\sigma_{by}} \right)_{\text{nominal}} = 25$

- Parameter List (PEPII SLAC Proposal)
- Plots for one pass
- Long Term Behavior { $\sigma_x, \sigma_y, L, \beta_y$ }
- Beam-Beam Tune Shift Limit
- Flip-Flop Instability

(1) Parameter List (SLAC Proposal).

Table 4-23. Main B Factory parameters used in the beam-beam simulation studies.

	LER (e^+)	HER (e^-)
E [GeV]	3.1	9
s_B [m]	1.26	1.26
f_c [MHz]	238	238
V_{RF} [MV]	8.0	18.5
f_{RF} [MHz]	476.0	476.0
ϕ_s [deg]	170.6	168.7
α	1.15×10^{-3}	2.41×10^{-3}
v_s	0.0403	0.0520
σ_t [cm]	1	1
N_b	5.61×10^{10}	3.88×10^{10}
ϵ_{0x} [nm-rad]	92	46
ϵ_{0y} [nm-rad]	3.6	1.8
β_x^* [cm]	37.5	75.0
β_y^* [cm]	1.5	3.0
σ_{0x} [μm]	186	186
σ_{0y} [μm]	7.4	7.4
τ_x [turns]	4400	5014
τ_y [turns]	4400	5014

$$\rightarrow L = 3 \times 10^{33} \text{ cm}^{-2}\text{s}^{-1}$$

$$\beta_{0x}^+ = \beta_{0y}^+ = \beta_{0x}^- = \beta_{0y}^- = 0.03$$

$$Q_x = 0.09, \quad Q_y = 0.06$$

(z) One pass

Equilibrium Beam Profile Before 1st Pass

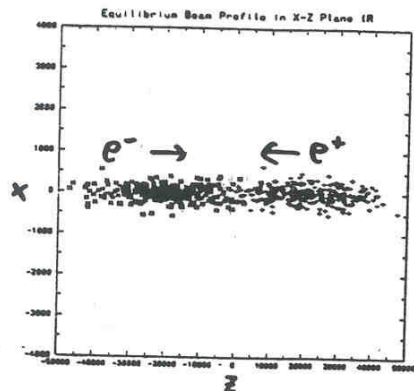


Figure 1: Initial beam profile in X-Z plane

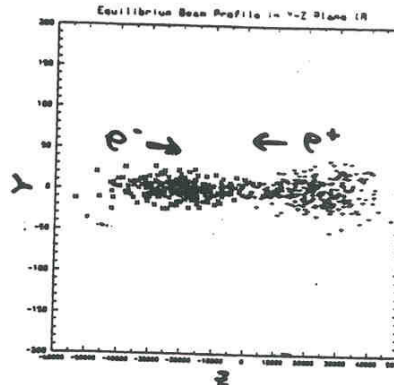


Figure 3: Initial beam profile in Y-Z plane

Longitudinal Charge Distribution

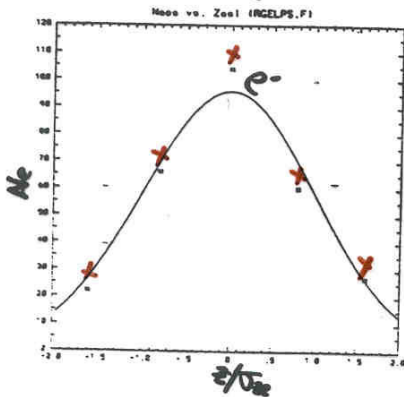


Figure 2: Longitudinal distribution of e^- macro-particles

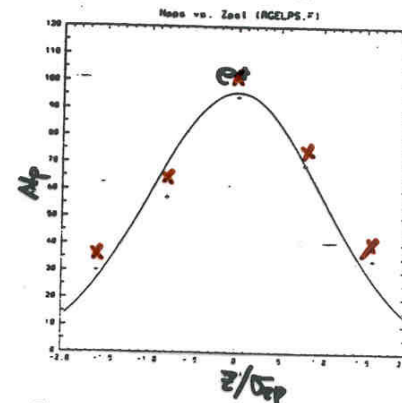


Figure 4: Longitudinal distribution of e^+ macro-particles

$$L_{\text{cal}} = 2.78 \times 10^{33}$$

$$L_0 = 3.02 \times 10^{33}$$

(3) Long Term Behavior (3 damping times)

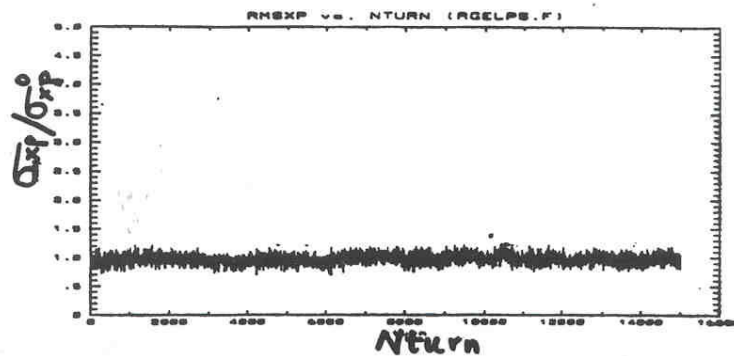


Figure 1: Horizontal blowup in three damping times

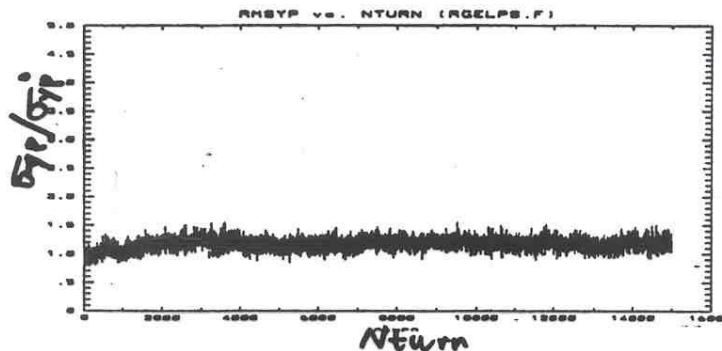


Figure 2: Vertical blowup in three damping times

For each given $\{N_e, N_p\}$, can obtain
a set of equilibrium $\{ \sigma_{x0}, \sigma_{y0}, \sigma_{xp}, \sigma_{yp}, \chi \}$

$$\{Q_x, Q_y\} = \{0.09, 0.06\}$$

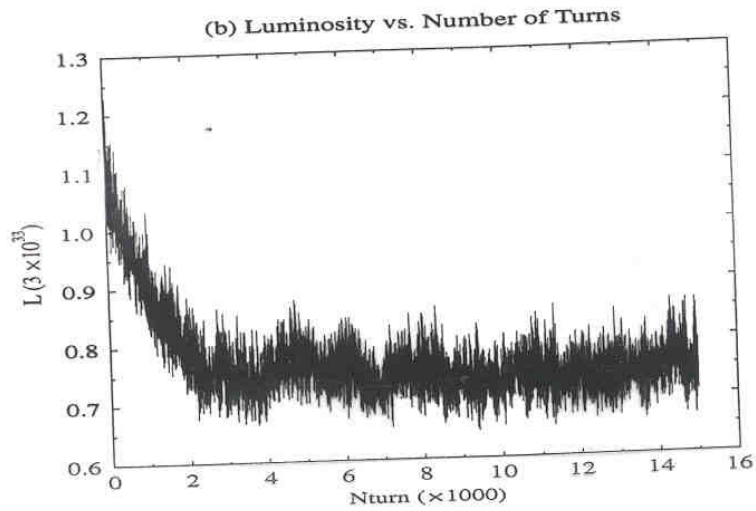
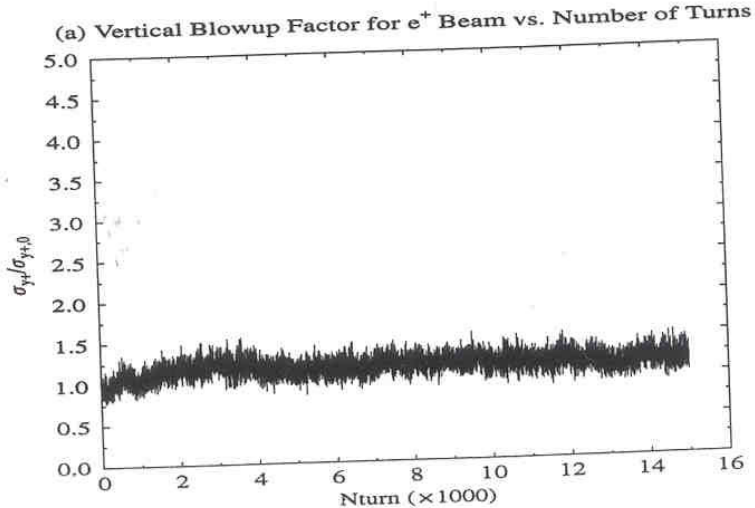
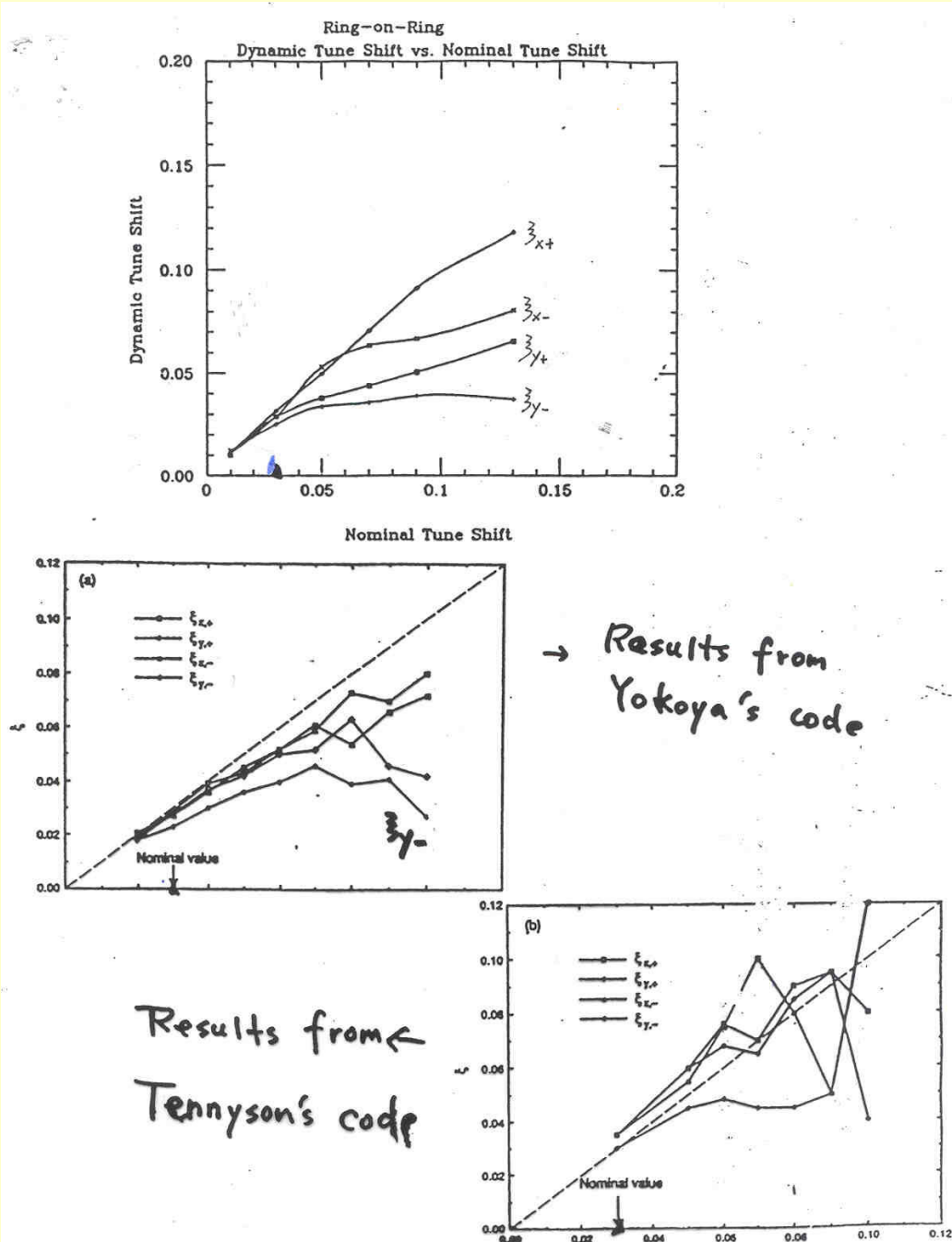


Figure 9: Beam blowup (a) and luminosity (b) for the positron beam during 15000 turns for parameters in Table 2.



(5)

Flip-Flop Effect in Storage Ring / Storage Ring



Coherent coupling
of transverse modes
in the two rings

This phenomenon was observed by R. Siemann and S. Krishnagopal using simulation which solves EM fields generated by round beams.

Our code allows general beam distribution \Rightarrow should be able to display the same effect.

Feature: at tunes just below quarter-integer, the beam distribution in the two rings oscillate in an anti-correlated manner between hollow and core with period 2.

(3) Linac-Ring Beam-Beam Effects

Simulation

$$\# \text{ of macroparticles in } \{e^-, e^+\} \text{ bunch} = \begin{cases} 360 \\ 1000 \end{cases}$$

$$\# \text{ of slices in } \{e^-, e^+\} \text{ bunch} = \begin{cases} 9 \\ 45 \end{cases}$$

$$\text{macrosize } \frac{\sigma_{mx,y}}{\sigma_{Bx,y}} = 0.5$$

$$\text{aspect ratio } R = \frac{\sigma_{mx}}{\sigma_{my}} = \left(\frac{\sigma_{Bx}}{\sigma_{By}} \right)_{\text{design}} = 3.93$$

- Parameter List (Sam Heifets)
- Plots for one pass
- Kink Instability
- Long Term Behavior
- Beam-Beam Tune shift Limit (w. and w/o matching)

(3) Linac-Ring Beam-Beam Effects

Simulation

$$\# \text{ of macroparticles in } \{e^-, e^+\} \text{ bunch} = \begin{cases} 360 \\ 1000 \end{cases}$$

$$\# \text{ of slices in } \{e^-, e^+\} \text{ bunch} = \begin{cases} 9 \\ 45 \end{cases}$$

macrosize $\frac{\sigma_{mx,y}}{\sigma_{Bx,y}} = 0.5$

aspect ratio $R = \frac{\sigma_{mx}}{\sigma_{my}} = \left(\frac{\sigma_{Bx}}{\sigma_{By}} \right)_{\text{design}} = 3.93$

- Parameter List (Sam Heifets)
- Plots for one pass
- Kink Instability
- Long Term Behavior
- Beam-Beam Tune Shift Limit (w. and w/o matching)

(3) Linac-Ring Beam-Beam Effects

Simulation

$$\# \text{ of macroparticles in } \{e^-, e^+\} \text{ bunch} = \begin{cases} 360 \\ 1000 \end{cases}$$

$$\# \text{ of slices in } \{e^-, e^+\} \text{ bunch} = \begin{cases} 9 \\ 45 \end{cases}$$

$$\text{macrosize } \frac{\sigma_{mx,y}}{\sigma_{Bx,y}} = 0.5$$

$$\text{aspect ratio } R = \frac{\sigma_{mx}}{\sigma_{my}} = \left(\frac{\sigma_{Bx}}{\sigma_{By}} \right)_{\text{design}} = 3.93$$

- Parameter List (Sam Heifets)
- Plots for one pass
- Kink Instability
- Long Term Behavior
- Beam-Beam Tune Shift Limit (w. and w/o matching)

(1) Parameter List (Sam Heifets)

B-Factory Parameter List by Heifets, et.al.

<i>Linac</i>	<i>Storage Ring</i>	<i>Collision</i>
$E_e = 3.5 \text{ GeV}$	$E_p = 8.0 \text{ GeV}$	$L = 10^{34} \text{ cm}^{-2} \text{ sec}^{-1}$
$N_e = 0.544 \times 10^9$	$N_p = 6.1 \times 10^{11}$	$D_{ey} = 273.7, D_{ez} = 69.6$
$I_{av} = 1.0 \text{ mA}$	$I_{ev} = 1.94 \text{ A}$	$\xi = 0.06$
$f_{RF} = 1.5 \text{ GHz}$	$n_B = 30$	$f_e = 20 \text{ MHz}$
$l_e^e = 2.2 \text{ psec}$	$s_B = 15 \text{ m}$	$\beta_{ey}^* = \beta_{pz}^* = 3.33 \text{ mm}$
$\epsilon_{ex} = 5.75 \text{ nm}, \epsilon_{ey} = 0.37 \text{ nm}$	$\epsilon_{px} = 5.75 \text{ nm}, \epsilon_{py} = 0.057 \text{ nm}$	$\beta_{py}^* = 21.55 \text{ mm}$
$P = 5.65 \text{ MW}$	$P = 15.1 \text{ MW}$	$\sigma_{ez}^D = \sigma_{pz}^* = 4.37 \mu\text{m}$
Power Loss = 2.0W/cav	$E' = 2.5 \text{ MeV/cavity}$	$\sigma_{ey}^D = \sigma_{py}^* = 1.11 \mu\text{m}$
$f_c = 20 \text{ MHz}$	$n_{cav} = 50$	
	$C = 450 \text{ m}$	
	$R_p = 10$	
	$\alpha = 2.0 \times 10^{-3}$	
	$\sigma_\delta = 2.45 \times 10^{-3}$	
	$\sigma_z^p = 3.33 \text{ mm}$	
	$\left(\frac{Z}{n}\right)_{tot} = 0.5 \text{ ohm}$	
	$\rho_{bend} = 45 \text{ m}$	
	$\tau_x = 0.9 \text{ msec}, \tau_y = 2.4 \text{ msec}$	
	$\tau_\delta = 6.9 \text{ msec}$	
	$L_{cell} = 5 \text{ m}$	
	$\beta_x = 9.8 \text{ m}, \beta_y = 1.4 \text{ m}$	
	$D_z = 0.255 \text{ m}$	

$$Q_s = 0.07$$

Choose $Q_x = 0.64, Q_y = 0.54$

$$\frac{T_x}{T_0} = 600, \frac{T_y}{T_0} = 1600, \frac{T_f}{T_0} = 4600$$

(z) Plots for One Pass

Beam Profile Before 1st pass After 1st pass

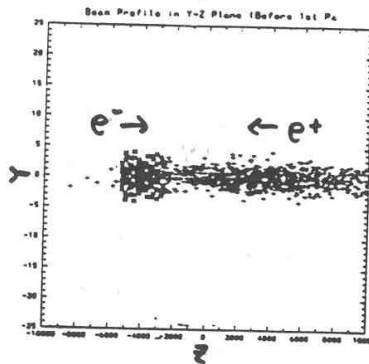


Figure 5: Initial beam profile in Y-Z plane

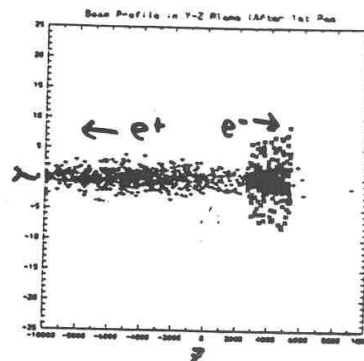


Figure 7: Beam profile in Y-Z plane after first collision

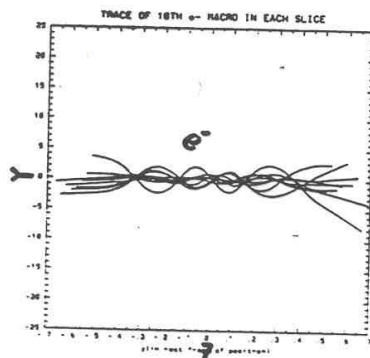


Figure 6: Trace of e^- particles in Y-Z plane in the rest frame of positron bunch

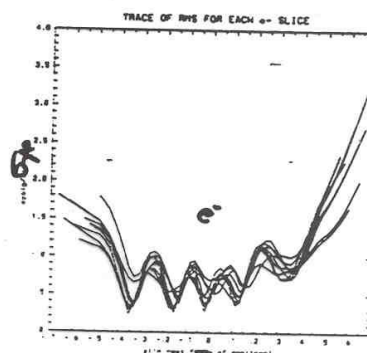


Figure 8: Trace of RMS for e^- slices in Y-Z plane in the rest frame of positron bunch

The deep modulation of e^- envelope
could have strong impact on
the stability of the positron bunch.

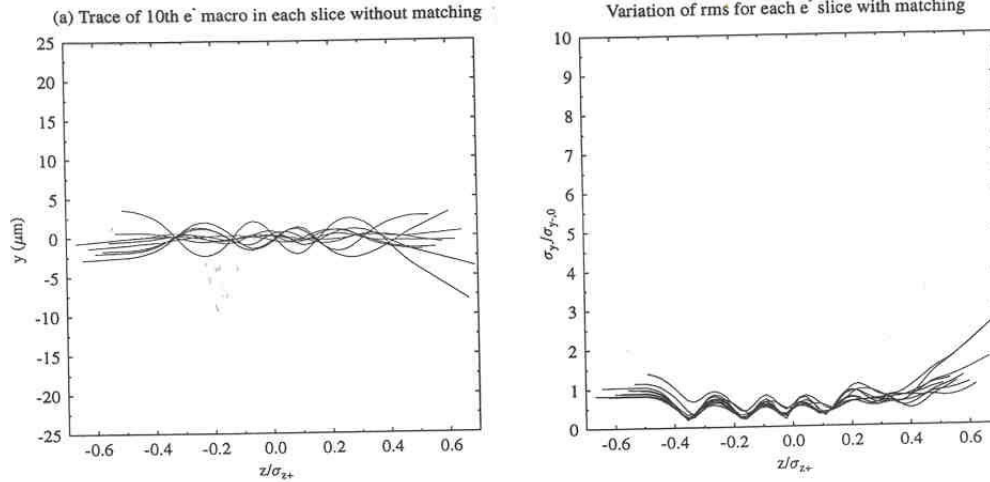


Figure 14: Trace of e^+ macros (a) and variation of rms for e^- slices (b) in Y-Z plane in the rest frame of the e^+ bunch *without* matching.

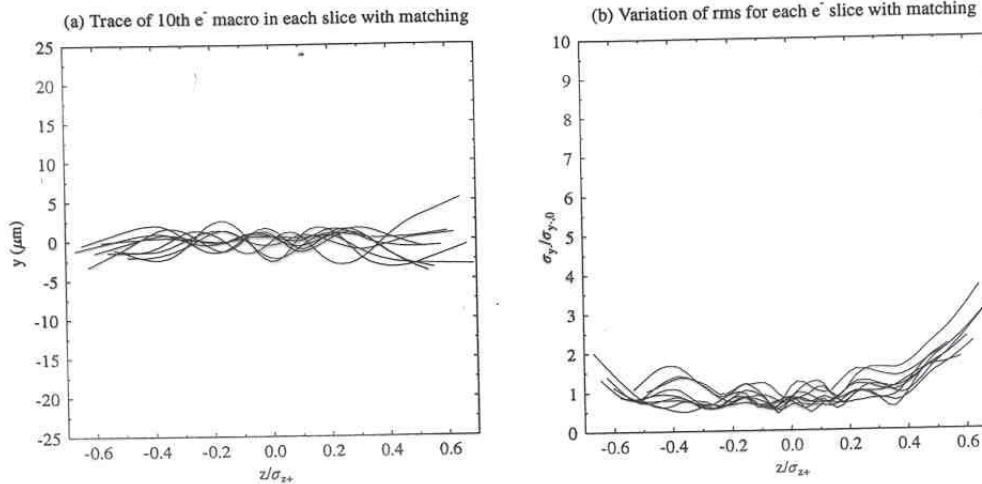
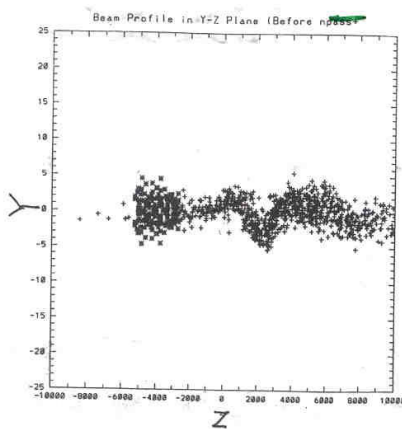


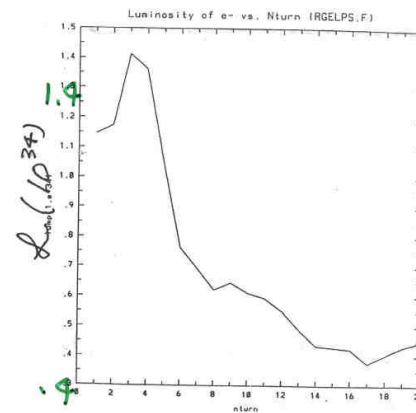
Figure 15: Trace of e^+ macros (a) and variation of rms for e^- slices (b) in Y-Z plane in the rest frame of the e^+ bunch *with* matching.

Kink Instability and Synchrotron Oscillation

Beam Profile after 20 turns

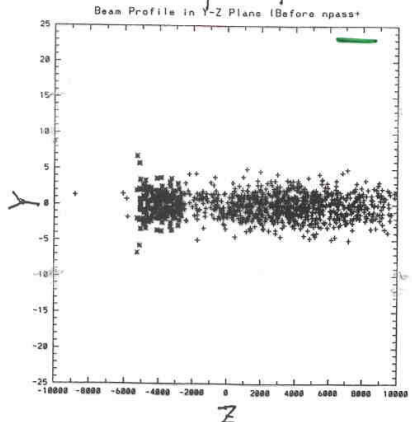


Luminosity vs. Nturn

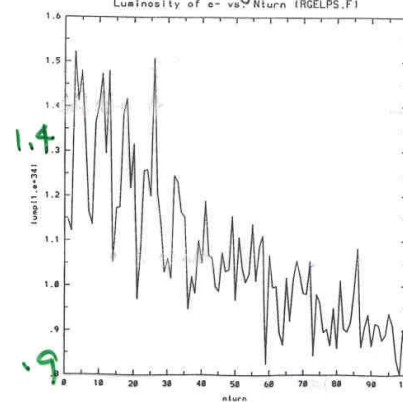


(a) beam-beam force + matrix. (random offset)

Beam Profile after 100 turns



Luminosity v. N-turn.



(b) beam-beam force + matrix + syn. osci. (random offset).
 $\boxed{\langle 2s = 0.07 \rangle}$

(3) Long Term Behavior

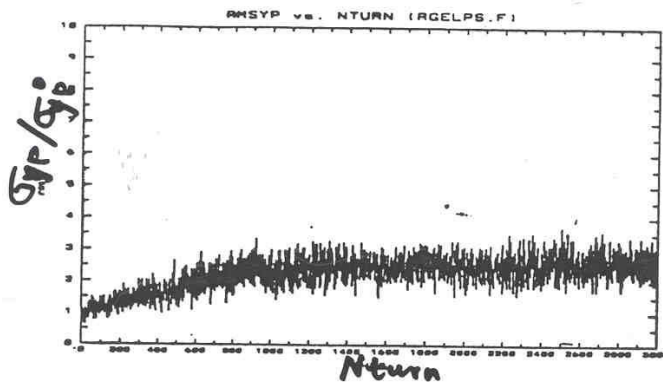


Figure 1: Positron beam blowup in 3000 turns

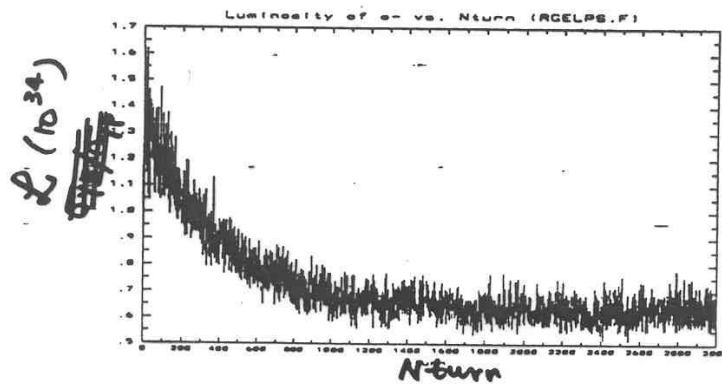
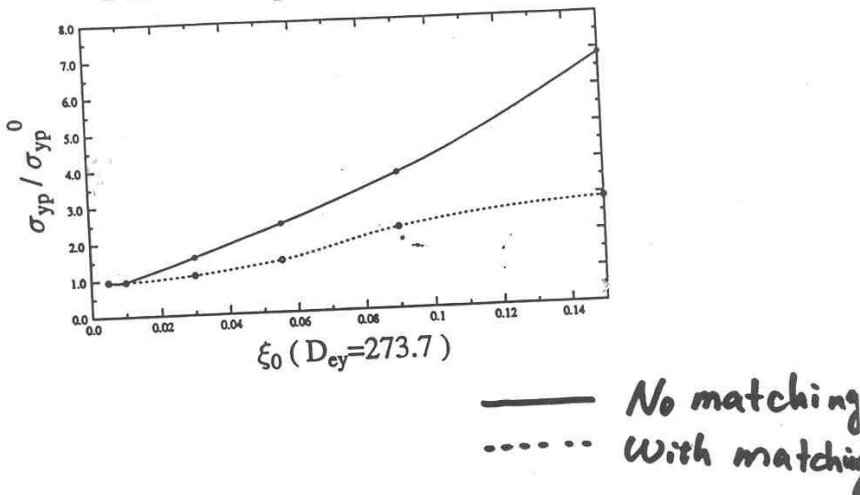


Figure 2: Luminosity in 3000 turns

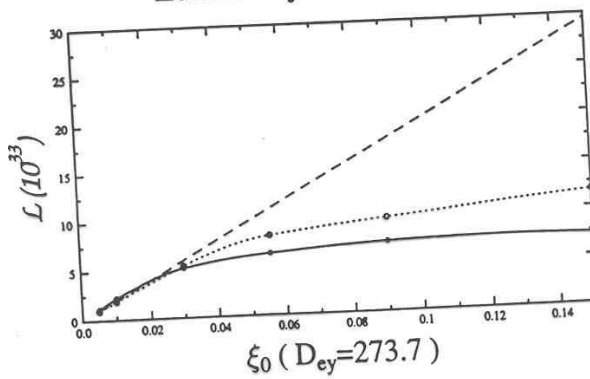
Given (N_+, N_-) , can obtain an equilibrium set
of $(\sigma_{x+}, \sigma_{y+}, L)$

(4) Beam-Beam Tune Shift limit

Beam Blowup Factor vs. Tune Shift



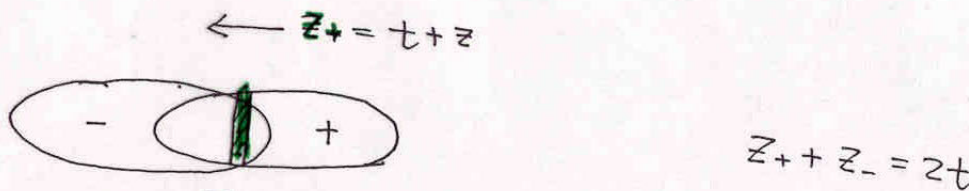
Luminosity vs. Tune Shift



$$(\nu_e, \nu_\mu) = (0.64, 0.54)$$

3. Analysis of Coherent Kink Instability

- Coherent growth of transverse displacement of e^+ beam
 - ribbon bunch model ($\sigma_x \gg \sigma_y$)
 - constant offset of the e^- beam for each collision
 - longitudinal uniform distribution



Coupled equations for vertical offsets of overlapping slices in e^-e^+ bunch

- Eq. of motion for \bar{y}_+ , \bar{y}_- ($c=1$)

$$\left\{ \begin{array}{l} \left(\frac{\partial}{\partial t} + \frac{\partial}{\partial z} \right)^2 \bar{y}_- = -k_-^2 [\bar{y}_- - \bar{y}_+] \\ \left(\frac{\partial}{\partial t} - \frac{\partial}{\partial z} \right)^2 \bar{y}_+ = -k_+^2 [\bar{y}_+ - \bar{y}_-] \end{array} \right.$$

with

$$k_-^2 = \alpha_- \frac{\lambda_+}{f_{y_-}}$$

$$k_+^2 = \alpha_+ \frac{\lambda_-}{f_{y_+}}$$

↑ using the linear part of beam-beam kick

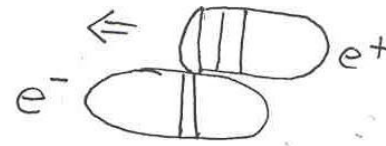
Coupled Equation of Motion (in comoving coordinates)

$$e^- \left\{ \begin{array}{l} \frac{d^2 \bar{y}_-(z_-, t)}{dt^2} + k_-^2 \bar{y}_-(z_-, t) = k_-^2 \bar{y}_+(z_+ = zt - z_-, t) \\ \frac{d^2 \bar{y}_-(z_-, t)}{dt^2} = 0 \end{array} \right. \quad \begin{array}{l} (0 < z_- < l_-) \\ \left(\frac{z_-}{z} \leq t \leq \frac{z_- + l_+}{z} \right) \end{array}$$

$$e^+ \left\{ \begin{array}{l} \frac{d^2 \bar{y}_+(z_+, t)}{dt^2} + k_+^2 \bar{y}_+(z_+, t) = k_+^2 \bar{y}_-(z_- = zt - z_+, t) \\ \frac{d^2 \bar{y}_+(z_+, t)}{dt^2} = 0 \end{array} \right. \quad \begin{array}{l} (0 < z_+ < l_+) \\ \left(\frac{z_+}{z} \leq t \leq \frac{z_+ + l_-}{z} \right) \end{array}$$

Using Laplace transform

For $\tau_- = t - \frac{z_-}{2}$:



- $$\bar{Y}_-(z_-, t = \tau_- + \frac{z_-}{2}) = \bar{Y}_-(z_-, t = \frac{z_-}{2}) \underset{=} {y_0} \cos k_- \tau_- + \bar{Y}'(z_-, t = \frac{z_-}{2}) \frac{\sin k_- \tau_-}{k_-}$$

$$+ k_- \int_0^{\tau_-} d\tau'_- \sin k_- (\tau_- - \tau'_-) \bar{Y}_+(z_+ = 2\tau'_-, t = \frac{z_-}{2} + \tau'_-)$$

$$(0 \leq z_- \leq l_-, 0 \leq \tau_- \leq \frac{l_+}{2})$$

For $\tau_+ = t - \frac{z_+}{2}$:

- $$\bar{Y}_+(z_+, t = \tau_+ + \frac{z_+}{2}) = \bar{Y}_+(z_+, t = \frac{z_+}{2}) \cos k_+ \tau_+ + \bar{Y}'(z_+, t = \frac{z_+}{2}) \frac{\sin k_+ \tau_+}{k_+}$$

$$+ k_+ \int_0^{\tau_+} d\tau'_+ \sin k_+ (\tau_+ - \tau'_+) \bar{Y}_-(z_- = 2\tau'_+, t = \tau'_+ + \frac{z_+}{2})$$

$$(0 \leq z_+ \leq l_+, 0 \leq \tau_+ \leq \frac{l_-}{2})$$

integral of kicks from e-slices

Integral Equation ($0 \leq z_+ \leq l_+$, $0 \leq \tau_+ \leq \frac{l_-}{z}$)

$$\bar{Y}_+(z_+, t = \tau_+ + \frac{z_+}{z}) = \bar{Y}_+^{(0)}(z_+, t = \tau_+ + \frac{z_+}{z}) + \int_0^{\tau_+} k_+ d\tau'_+ \sin k_+(\tau_+ - \tau'_+) \int_0^{z_+} \frac{k_-}{z} dz'_+ \sin \frac{k_-(z_+ - z'_+)}{z} \bar{Y}_+(z'_+, t = \tau'_+ + \frac{z'_+}{z})$$

$\sim \Lambda \bar{y}_+()$

with initial conditions:

$$\bar{Y}_+^{(0)}(z_+, t = \tau_+ + \frac{z_+}{z}) = \bar{Y}_+(z_+, t = \frac{z_+}{z}) \cos k_+ \tau_+ + \bar{Y}'_+(z_+, t = \frac{z_+}{z}) \frac{\sin k_+ \tau_+}{k_+} + Y_0 \cos \frac{k_- \tau_+}{z} (1 - \cos k_+ \tau_+)$$

- For $\Lambda = \left(\frac{k_+ l_-}{z}\right)^2 \frac{k_- l_+}{z} \ll 1$ (example: $\frac{k_+ l_-}{z} \approx 0.1$, $\frac{k_- l_+}{z} = 17$,) $\Lambda = 0.17$
- \Rightarrow First order iteration

Multipass

$$X_N \approx -\frac{\lambda N}{(1-\eta_1)(\eta_1-\eta_2)} M_2 (M^{(B)})^{N-2} [O(M^{(B)} A) ..]$$

$$X_{n+1} = M^{(R)} [M^{(B)} X_n + A + \lambda O(X_n) + \lambda P(A)]_1]$$

$$M^{(R)} = \begin{pmatrix} \cos 2\pi \gamma_B & \beta^* \sin 2\pi \gamma_B \\ -\frac{1}{\beta^*} \sin 2\pi \gamma_B & \cos 2\pi \gamma_B \end{pmatrix}$$

In the regime of initial linear growth,
for $X_0 = 0$, $M^{(R)} = I$.

$$\boxed{\bar{Y}_+(z_+, t_N) = -y_0 N \left(\frac{k+l_-}{4}\right) \left(\frac{k_+ z_+}{4}\right) \sin \frac{k+l_-(N-\frac{3}{2})}{2} \sin \frac{k_- z_+}{2}}$$

— Sinusoidal oscillation in both space and time

$$|\bar{Y}_+| \propto N \cdot z_+$$

Previous Observation in Simulation of Linac-Ring B factory

e^-	e^+	Collision
$E_e = 2 \text{ GeV}$	$E_p = 10 \text{ GeV}$	$L_0 = 5.42 \times 10^{34} \text{ cm}^{-2} \text{ sec}^{-1}$
$N_e = 0.5 \times 10^9$	$N_p = 10^{12}$	$D_{ey} = 90, D_{py} = 0.01$
$l_e = 500 \mu\text{m}$	$l_p = 500 \mu\text{m}$	$y_0 = y_{\text{offset}} = 0.1 \mu\text{m}$
$\sigma_{ey} = 0.3 \mu\text{m}$	$\sigma_{py} = 0.3 \mu\text{m}$	
$\sigma_{ex} = 3 \mu\text{m}$	$\sigma_{px} = 3 \mu\text{m}$	

Table 1: Parameter List in Simulation

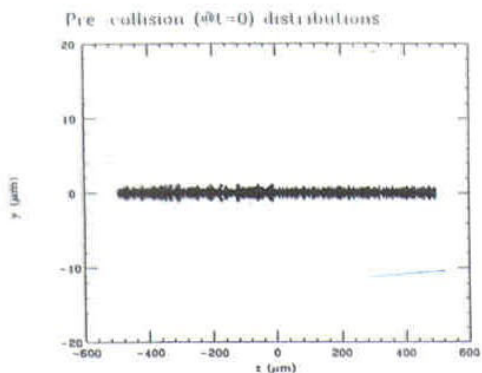


Figure 3: Pre-collision distribution in the simulation for the first collision, with $z < 0$ for the electron bunch and $z > 0$ for the positron bunch, modeled by 2000 macro-particles in 50 slices for each bunch. The offset is $y_0 = 0.1 \mu\text{m}$.

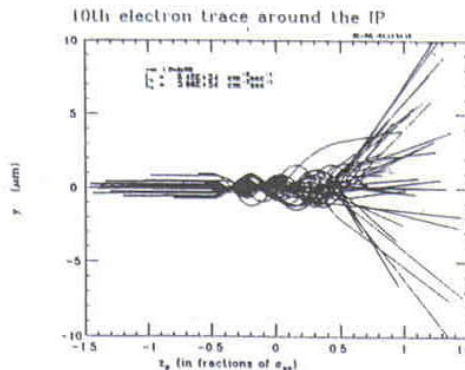


Figure 4: Trace of 10th macro-particle in each slice of the electron bunch, plotted in the rest frame of the positron bunch

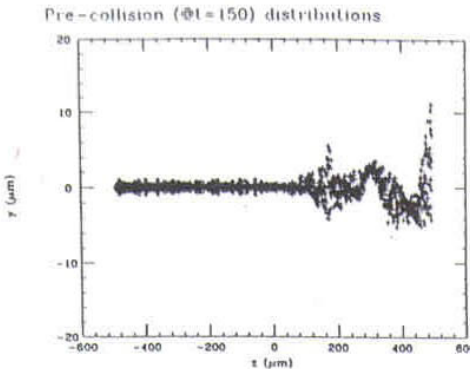


Figure 5: Pre-collision distribution in the simulation for 150th collision, with $z < 0$ for the electron bunch and $z > 0$ for the positron bunch. The offset is $y_0 = 0.1 \mu\text{m}$ for every collision.



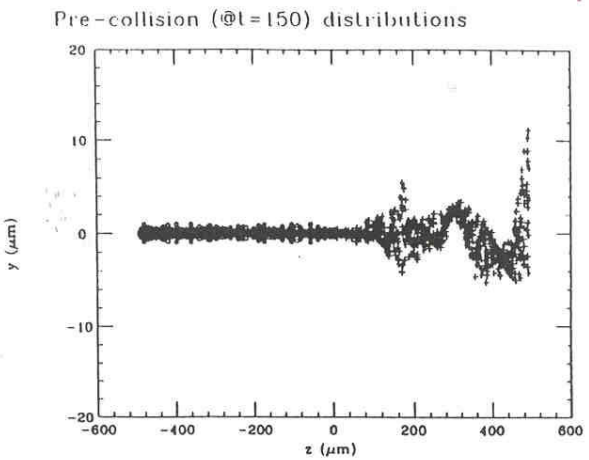


Figure 5: Pre-collision distribution in the simulation for 150th collision, with $z < 0$ for the electron bunch and $z > 0$ for the positron bunch. The offset is $y_0 = 0.1\mu\text{m}$ for every collision.

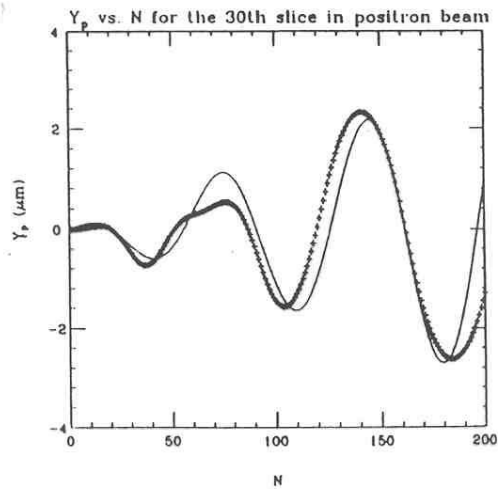


Figure 6: Comparison of analytical results (solid curve) with numerical results (dotted curve) for Y_p vs. collision number N with $z_p/l_p = 0.6$.

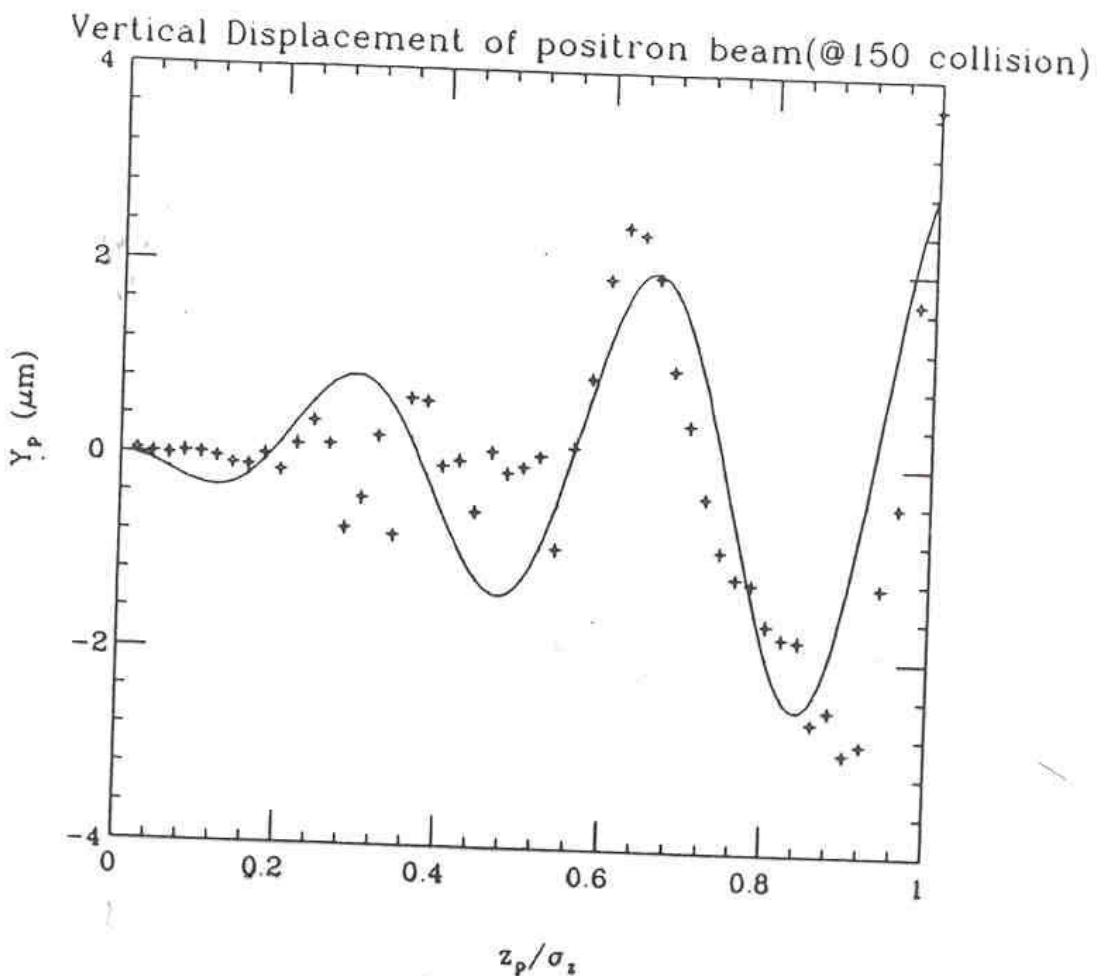


Figure 7: Comparison of analytical results (solid curve) with numerical results (dotted curve) for Y_p vs. the longitudinal distance z_p at the pre-collision state for $N = 150$.

Recent Design of Linac-Ring Electron-Ion Collider

AN ENERGY RECOVERY ELECTRON LINAC-ON-PROTON RING COLLIDER

L. Merminga, G. A. Krafft, Jefferson Lab, Newport News, VA 23606, USA

V. A. Lebedev, FNAL, Batavia, IL 60510, USA



Figure 1. Schematic layout of the electron linac – proton ring collider.

Table 1: Parameter table for linac-ring scenarios

Parameter	Units	Design 1	Design 2
E_e	GeV	5	5
E_p	GeV	50	50
N_e	ppb	1.1×10^1 0	1.1×10^{10}
N_p	ppb	1.0×10^1 1	1.0×10^{11}
f_c	MHz	150	150
σ_e^*	μm	25	25
σ_p^*	μm	60	25
ε_e	nm	6	6
ε_p	nm	36	6.25
β_e^*	cm	10	10
β_p^*	cm	10	10
σ_z^p	cm	10	10
σ_z^e	mm	1	1
ξ_p	–	.004	.004
Δv_L	–	.004	.024
D_e	–	.78	4.6
I_e	A	.264	.264
I_p	A	2.4	2.4
L	$\text{cm}^2\text{sec}^{-1}$	6.2×10^{32} π^2	2.1×10^{33}



4. Strong Head-Tail Instability in a Linac-Ring e-p Collider

Assumptions: Linear beam-beam force
very short e bunch

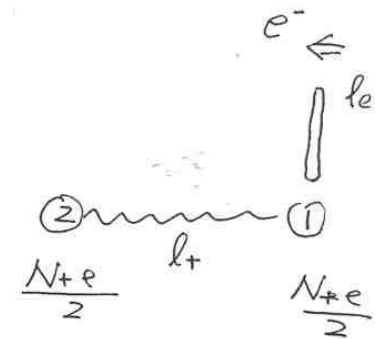
(betatron phase variation in IR is not yet included: $l_+ \ll \beta_{y+}^*$)

- Two Particle (or Slice) Model
- Vlasov Analysis



Two - Macroparticle Model

- Particle "1" of the proton beam with offset y_1 will kick the electron bunch centroid



$$\Delta y'_- = \frac{y_1}{4f_-} \quad \left(f_-^{-1} = \frac{2N_p r_e}{\gamma_- \bar{\sigma}_{y+} (\bar{\sigma}_{x+} + \bar{\sigma}_{y+})} \right)$$

- Particle "2" at l_+ behind "1" sees e^- bunch offset

$$\Delta y_- = \Delta y'_- \cdot l_+$$

- The e^- bunch then kick "2" by

$$\Delta y'_+ = \frac{\Delta y_- - y_2}{2f_+} \quad \left(f_+^{-1} = \frac{2N_e r_i}{\gamma_+ \bar{\sigma}_{y-} (\bar{\sigma}_{x-} + \bar{\sigma}_{y-})} \right)$$

$$\text{For } k_+^2 = \frac{1}{2f+C} \ll k_\beta^2, \quad \alpha^2 = \frac{\ell_+}{8f+f-C} \propto D\beta_+$$

$$\begin{cases} y_1'' + k_\beta^2 y_1 = 0 \\ y_2'' + k_\beta^2 y_2 = \alpha^2 y_1 \end{cases}$$

$$\text{Let } \tilde{y}_{1,2} = y_{1,2} + i \frac{1}{k_\beta} y_{1,2}', \quad \Gamma = \frac{\pi \alpha^2}{2k_\beta k_s}$$

$$\begin{bmatrix} \tilde{y}_1 \\ \tilde{y}_2 \end{bmatrix}_{s=\frac{C_s}{2}} = e^{-i \frac{k_\beta C_s}{2}} \begin{bmatrix} 1 & 0 \\ i\Gamma & 0 \end{bmatrix} \begin{bmatrix} \tilde{y}_1 \\ \tilde{y}_2 \end{bmatrix}_{s=0}$$

After $s = \frac{C_s}{2}$, "1" and "2" switch role,

$$\begin{bmatrix} \tilde{y}_1 \\ \tilde{y}_2 \end{bmatrix}_{s=C_s} = e^{-i \frac{k_\beta C_s}{2}} \begin{bmatrix} 1 & i\Gamma \\ 0 & 1 \end{bmatrix} e^{-i \frac{k_\beta C_s}{2}} \begin{bmatrix} 1 & 0 \\ i\Gamma & 1 \end{bmatrix} \begin{bmatrix} \tilde{y}_1 \\ \tilde{y}_2 \end{bmatrix}$$

$\underbrace{\qquad\qquad\qquad}_{M}$

Stability Criteria:

$$|M - \lambda I| = 0, \quad |\lambda| \leq 1$$

$$\Rightarrow \Gamma \leq 2, \quad \text{or} \quad \frac{D - \beta_+}{\omega_s} \leq \frac{16}{\pi} \left(\frac{\beta_{z+}}{\ell_+} \right)$$

(choice of ℓ_+ is somewhat arbitrary).

Example:

$$\beta_+ = 0.004, \quad \omega_s = 3 \times 10^{-4}, \quad D = 0.78, \quad \frac{\beta_+ D}{\omega_s} = 10$$

$$D = 4.6, \quad \frac{\beta_+ D}{\omega_s} = 61$$

Two Particle Model vs. Vlasov Analysis

Two Particle Model:

- Gives clear picture of the interaction mechanism and cause of instability
- Overlooked the behavior of beam-beam kick from electron slice on the ion bunch along the ion bunch length
- Simplified the localized beam-beam kick as distributed interaction

Vlasov Analysis:

- Consider dynamics of vertical dipole moments of a ribbon ion bunch in a storage ring colliding with a ribbon electron bunch from linac
- Hourglass effect on synchrobetatron coupling is not included $l_+ \ll \beta_{y+}^*$
- Electron bunch is described by delta-like slice $l_- \ll l_+$
- Uniform longitudinal charge distribution $\lambda_{z+} = 1/l_+$



Operated by the Southeastern Universities Research Association for the U.S. Dept. of Energy

Dynamics of the Stored Ion Beam

- Equation of motion for an ion particle: ($k_\beta = \omega_\beta / c, k_s = \omega_s / c, C$: circumference of the ring)

$$\begin{cases} \frac{dy}{ds} = u_y \\ \frac{du_y}{ds} + k_\beta^2 y = -\underbrace{\frac{y - \bar{y}}{f_+} \sum_{n=0}^{\infty} \delta(s - z/2 + nC)}_{\frac{F_y(z,s)}{E}} \\ \frac{dz}{ds} = -\eta \delta \\ \frac{d\delta}{ds} = k_s^2 z / \eta \end{cases}$$

- Vlasov equation for the distribution function $g(y, u_y, z, \delta, s)$

$$\frac{\partial g}{\partial s} + u_y \frac{\partial g}{\partial y} + \frac{F_y(z, s)}{E} \frac{\partial g}{\partial u_y} + (-\eta \delta) \frac{\partial g}{\partial z} + \frac{k_s^2 z}{\eta} \frac{\partial g}{\partial \delta} = 0$$

- Using action-angle transformation, we have for $f(q, \theta, r, \varphi, s)$

$$\begin{cases} y = q \cos \theta \\ u_y = -k_\beta q \sin \theta \end{cases} \quad \begin{cases} z = r \cos \varphi \\ \frac{\eta \delta}{k_s} = r \sin \varphi \end{cases}$$

$$\frac{\partial f}{\partial s} + k_\beta \frac{\partial f}{\partial \theta} + k_s \frac{\partial f}{\partial \varphi} + \frac{F_y(z, s)}{E} \frac{\partial f}{\partial u_y} = 0$$



Analysis of Dipole Motion Using Linearized Vlasov Equation

- Linear beam-beam interaction force
- Neglecting hourglass effect
- Using action-angle transformation, we have for $f(q, \theta, r, \varphi, s) = f_0(q)g_0(r) + f_1(q, \theta, r, \varphi, s)$

$$\begin{cases} y = q \cos \theta \\ u_y = -k_\beta q \sin \theta \end{cases} \quad \begin{cases} z = r \cos \varphi \\ \frac{\eta}{k_s} \delta = r \sin \varphi \end{cases} \quad f_1(q, \theta, r, \varphi, s) = -\frac{\partial f_0}{\partial q} [e^{i\theta} g_+(r, \varphi, s) + e^{-i\theta} g_-(r, \varphi, s)]$$
$$g_{\pm}(r, \varphi, s) = \sum_{l=-\infty}^{\infty} R_l^{\pm}(r, s) e^{il\varphi}$$

$$\frac{\partial f_1}{\partial s} + k_\beta \frac{\partial f_1}{\partial \theta} + k_s \frac{\partial f_1}{\partial \varphi} + \frac{F_y(z, s)}{E} g_0(r) \frac{\partial f_0}{\partial u_y} = 0$$

- Analogy to the broad band transverse wake function and impedance

$$\frac{F_y(z, s)}{E} = -\sum_{n=0}^{\infty} \delta(s - \frac{z}{2} - nC) \frac{y_+ - \bar{y}_-(z, s)}{f_*}, \quad \bar{y}_-(z, s) = \frac{z}{2} + nC = \frac{k_- c}{2} \int_{-\infty}^z dz' W^\perp(z - z') \bar{y}_+(z', s' = nC),$$

$$W^\perp(z) = \sin \frac{k_- z}{2} H(z), \quad \begin{cases} \text{Re} Z^\perp = \frac{\pi}{2} \left[\delta(\omega - \frac{k_- c}{2}) - \delta(\omega + \frac{k_- c}{2}) \right] \\ \text{Im} Z^\perp = \frac{k_- c}{4\omega} \left[\frac{1}{\omega - \frac{k_- c}{2}} + \frac{1}{\omega + \frac{k_- c}{2}} \right] \end{cases}$$



Equation for Single Collision

- Expansion in terms of modes for a uniform bunch distribution

$$R_l^\pm(r, s) = W_0(r) \sum_{M=0}^{\infty} a_{lm}^\pm(s) h_m^{[l]}(r)$$

$$h_m^{[l]}(r) = \sqrt{4\pi} \frac{(|l|+2m+1/2)m!\Gamma(|l|+m+1/2)}{(|l|+k)!\Gamma(m+1/2)} \left(\frac{r}{\hat{z}}\right)^{|l|} P_m^{(|l|-1/2)} \left(1 - \frac{r^2}{2\hat{z}^2}\right)$$

- Equation for a_{lm}^\pm before and after a single collision:

$$\begin{cases} a_{lm}^{(+)} - a_{lm0}^{(+)} = \sum_{l',m'} M_{lm,l'm'} a_{l'm'}^{(+)} - a_{lm0}^{(+)} \\ a_{lm}^{(-)} - a_{lm0}^{(-)} = - \sum_{l',m'} M_{lm,l'm'} a_{l'm'}^{(+)} - a_{lm0}^{(+)} \end{cases}$$

- Coupling matrix

$$M_{lm,l'm'} = \underbrace{i^{l-l'} [\text{sign}(l)]' [\text{sign}(l')]'}_{c_{l,l'}} \int_{-\infty}^{\infty} dk [Z^\perp(k)c] g_{|l|m}(k) g_{|l'|m'}(k),$$

$$g_{|l|m}(k) = \sqrt{\frac{(|l|+2m+1)\Gamma(m+1/2)\Gamma(|l|+m+1/2)}{2\pi m!(|l|+m)!}} \frac{J_{|l|+2m+1/2}(k\hat{z})}{\sqrt{k\hat{z}}}$$



Stability Analysis

- Equation for a beam-beam interaction and ring transport

$$\begin{pmatrix} a_{lm}^{(+)} \\ \vdots \\ a_{lm}^{(-)} \\ \vdots \end{pmatrix}_{n+1} = \underbrace{\begin{pmatrix} e^{-i\mu_\beta} & & & \\ & \ddots & 0 & \\ & 0 & e^{i\mu_\beta} & \\ & & & \ddots \end{pmatrix}}_{\Xi} \begin{pmatrix} e^{i\mu_s} & & & \\ & \ddots & 0 & \\ & 0 & e^{i\mu_s} & \\ & & & \ddots \end{pmatrix} \begin{pmatrix} I + M & M \\ -M & I - M \end{pmatrix} \begin{pmatrix} a_{lm}^{(+)} \\ \vdots \\ a_{lm}^{(-)} \\ \vdots \end{pmatrix}_n$$

- Expression for coupling matrix M

$$M_{lm,l'm'} = c_{l,l'} \pi \xi_+ \chi \left[c_{\text{odd}} J_\mu(\chi) J_{\mu'}(\chi) + i c_{\text{even}} \left(\frac{(-)^{(\mu-\mu')/2}}{\sin \frac{(\mu+\mu')\pi}{2}} J_{\max(\mu,\mu')}(\chi) J_{-\min(\mu,\mu')}(\chi) - \frac{4}{\pi^2} \frac{2}{\mu^2 - \mu'^2} \right) \right]$$

with $\mu = |l| + 2m + 1/2, \mu' = |l'| + 2m' + 1/2,$

$$c_{\text{odd}} = (1 + (-)^{|l|+|l'|+1})/2, \quad c_{\text{even}} = (1 + (-)^{|l|+|l'|})/2$$

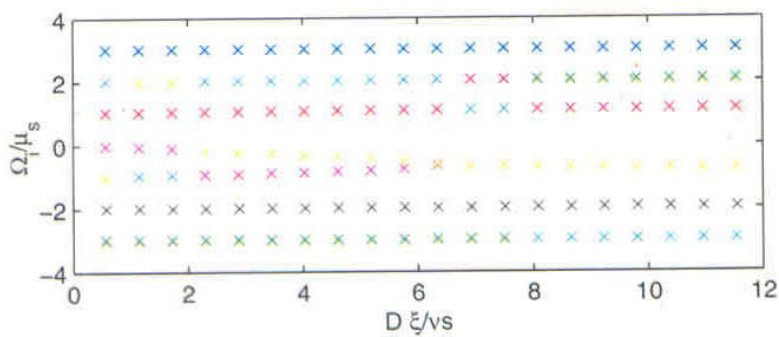
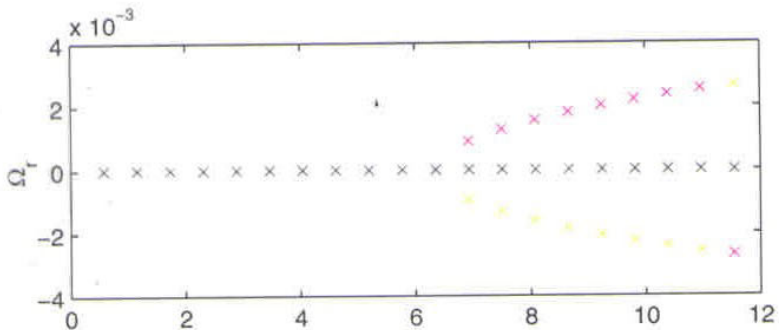
- Stability requires:

$$|\Xi - \lambda I| = 0, \quad \lambda = e^{\Omega_r + i\Omega_i}, \quad \Omega_r \leq 0$$



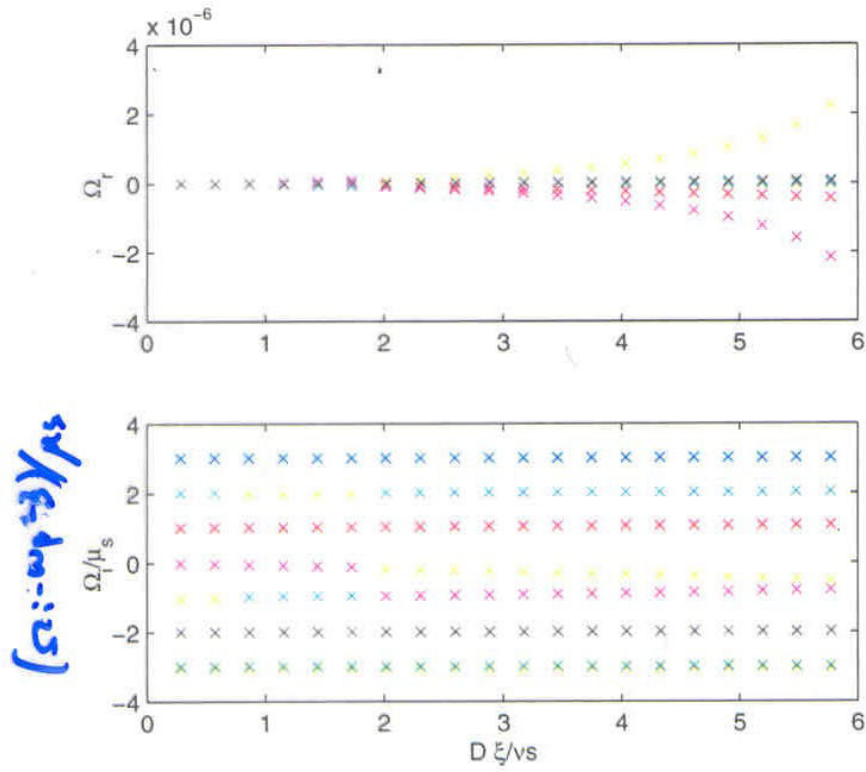
Transverse Mode Coupling

Ω_r and Ω_i/μ_s vs. $D_- \xi_+/\nu_s$ by varying ξ_+ for $\bar{D}_- = 4$ and $\nu_s = 0.001$



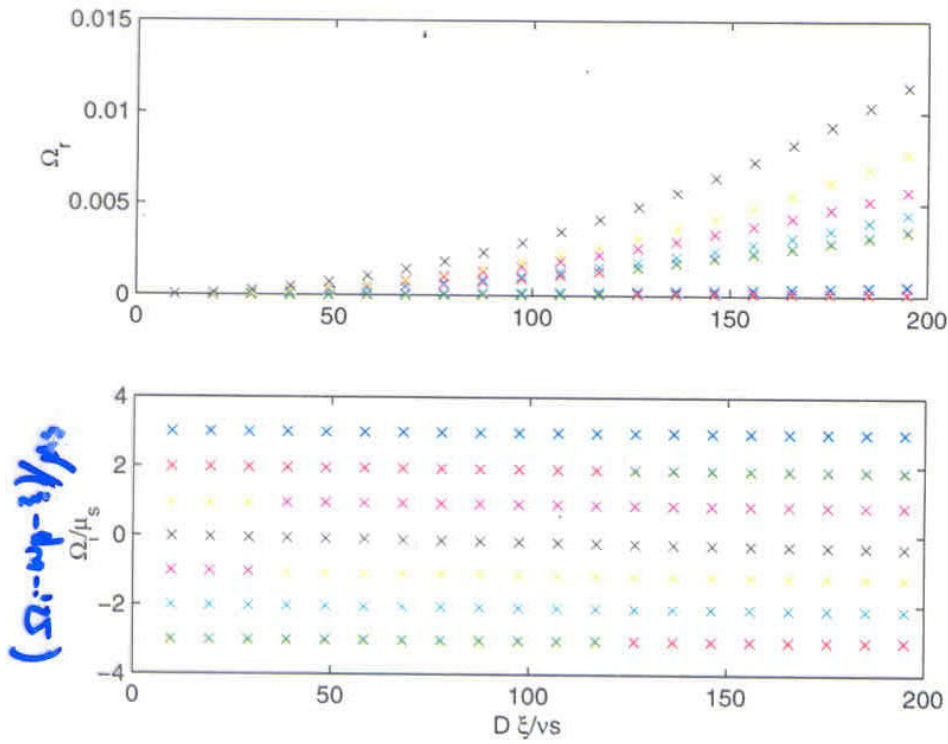
Operated by the Southeastern Universities Research Association for the U.S. Dept. of Energy

Small Growth Rate in the “Stable” Region



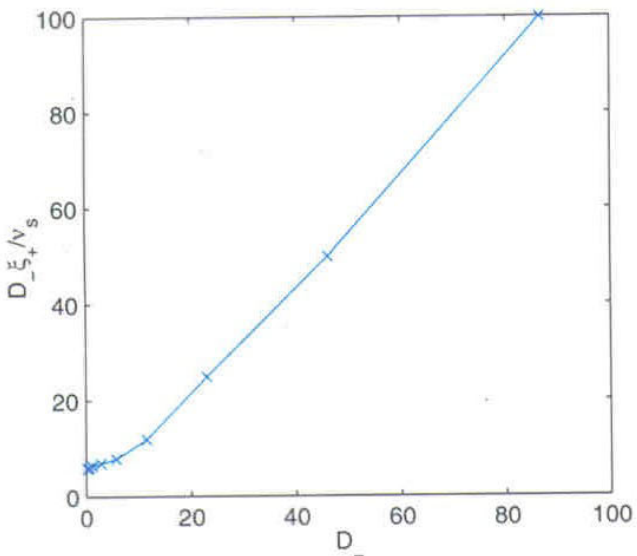
Growth Rate for Highly Disruption Case

Mode growth for ξ_+ from 0 to 0.05 while fixing $D_- = 273$ and $v_s = 0.07$, which are parameters used in our earlier study of linac - ring B factory



Threshold vs. Disruption

- For higher disruption, the electron oscillate through the ion bunch, the kink instability threshold depends weaker on the disruption parameter.



Conclusion

- A Strong-strong beam-beam simulation was earlier developed to study beam-beam effects in a linac-ring B factory, and is recently modified to study beam-beam effects in a linac-ring EIC.
- Both simulation and analysis showed kink instability with bunch length effect for a linac-ring collider. Analysis was based on linear beam-beam force approximation.
- Head-tail effect due to betatron phase change in the IR for linac-ring beam-beam was studied by Perevedentsev [PRST 4, 024403 (2001)] and later by Yunn [Jlab-TN-01-017], which is not yet included in the present Vlasov analysis.
- For the head-tail and strong head-tail instability analysis, we need to include effects of full nonlinearity of beam-beam interaction, and compare with simulation.

